spin wave linewidth and on the power in the saturating signal; the theory agrees well with observation.

This work has obvious applications to radar systems, especially where the frequency is swept; it also provides a novel and sensitive way to determine spin wave linewidths.

ACKNOWLEDGMENT

The authors wish to thank Dr. R. W. Patterson for his advice during this enquiry.

REFERENCES

[1] R. Orth, "Frequency selective limiters and their applications," *IEEE Trans. Electromag. Compat.*, vol. EMC-10, pp. 273–283, 1968.
[2] H. Suhl, "The theory of ferromagnetic resonance at high signal powers," *J. Phys. Chem. Sol.*, vol. 1, pp. 209–227, 1957.
[3] J. L. Carter and J. W. McGowan, "A laminary subsidiary resonance limiter," *IEEE Trans. Microwave Theory Tech.*, vol. MTT-18, pp. 652–654, 1970.
[4] R. C. Fletcher, R. C. LeCraw, and E. G. Spencer, "Electron spin relaxation in ferromagnetic insulators," *Phys. Rev.* vol. 117, pp. 955–963, 1960.
[5] E. Schlömann, T. J. Green, and U. Milano, "Recent developments in ferromagnetic resonance at high power levels," *J. Appl. Phys.*, vol. 31, pp. 386S–395S, 1960.

Computer-Aided Synthesis of the Optimum Refractive-Index Profile for a Multimode Fiber

KATSUNARI OKAMOTO AND TAKANORI OKOSHI, MEMBER, IEEE

***Abstract*—In a multimode optical fiber, the so-called multimode dispersion (mode-delay difference) is the principal cause that widens the transmitted pulse. The multimode dispersion can be controlled by the refractive-index profile. However, the optimum profile that minimizes the multimode dispersion has not yet been determined.**

This paper describes the computer-aided trial-and-error synthesis of the optimum refractive-index profile. It is shown that the group delay is reduced to about 10^{-3} times the value obtained with the uniform core fiber, to about 10 ps/km. This value is comparable to the material dispersion obtained with an ordinary fused-silica fiber and a typical semiconductor laser. It is also shown that the optimum profile is a smoothed W-shaped one.

I. INTRODUCTION

SEVERAL types of permittivity profiles have been proposed as the optimum profile that minimizes the multimode dispersion (mode-delay difference) of an optical fiber [1]–[4]. In those proposals, however, the permittivity in the core is assumed to be proportional to r^α, where r is the radial coordinate and α is an arbitrary positive quantity. Therefore, the obtained profile cannot be the genuine optimum.

This paper describes an approach to the genuine optimum. We express the permittivity in the core by a power series in terms of r, and use the variational method [5] to obtain the delay time of each propagation mode. Next we compute the variance of the delay time, i.e., the group delay. Then we modify the permittivity profile so as to decrease the group delay toward its minimum. We repeat the aforementioned process of analysis, estimation, and modification until we obtain the optimum permittivity profile with which the group delay is minimized. The whole process of such trial-and-error synthesis is performed in the computer.

The example of the synthesis described in Section V of this paper is the synthesis of the optimum profile for a fiber in which ten LP modes propagate. The same method can, of course, be used for any number of modes. It is shown that the group delay can be reduced to about 10^{-3} times the value obtained with the uniform core fiber, to about 10 ps/km, and that the optimum profile is a smoothed W-shaped one. This result substantiates the validity of the proposals made by Suematsu and Furuya for slab waveguides [6] and the present authors [3].

II. RESTRICTING CONDITIONS

We assume that the refractive-index distribution is axially symmetric, and that the quantities listed as follows remain constant in the course of the optimization:

1) wavelength of light λ;
2) the maximum refractive index n_1 in the core and the refractive index in the cladding n_2;
3) number of propagating LP modes M.

Note that the core radius a is not fixed. The relative difference of the refractive indices, which is defined conventionally as

$$\Delta = \frac{(n_1{}^2 - n_2{}^2)}{2n_1{}^2} \doteqdot \frac{(n_1 - n_2)}{n_1} \tag{1}$$

also remains constant from the preceding condition (2).

Manuscript received March 26, 1976; revised July 19, 1976.
The authors are with the Department of Electronic Engineering, University of Tokyo, Bunkyo-Ku, Tokyo 113, Japan.

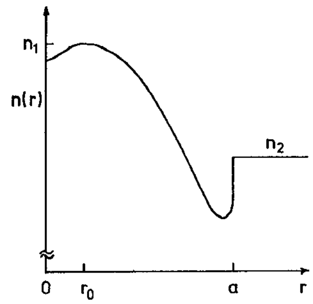

Fig. 1. Refractive-index profile of radially inhomogeneous optical fiber.

Next, we express the refractive index as

$$n^2(r) = \begin{cases} n_1{}^2[1 - 2\Delta g(r)], & 0 \le r \le a \\ n_2{}^2 = n_1{}^2[1 - 2\Delta], & r > a \end{cases} \tag{2}$$

where

$$g(r) = \sum_{p=1}^{n} \kappa_p \left[\left(\frac{r}{a}\right)^{2p} - \left(\frac{r_0}{a}\right)^{2p}\right] \tag{3}$$

and r_0 is the radius where $n(r)$ is highest (see Fig. 1). The coefficients κ_p $(p = 1,2,\cdots,n)$ are the parameters representing the refractive-index profile. Our aim is to determine the optimum set of κ_p.

III. Analysis of an Optical Fiber Using Variational Method

The first step in the trial-and-error synthesis is the analysis of a given fiber. A method of analysis based upon the variational principle [5] will be briefly described.

A. Propagation Constant

The propagation constant β of an axially symmetric optical fiber is expressed as [7]

$$\beta^2 = \frac{\int_0^\infty \int_0^{2\pi} k^2 n^2(r)|\Psi|^2 r\, dr\, d\theta - \int_0^\infty \int_0^{2\pi} |\nabla\Psi|^2 r\, dr\, d\theta}{\int_0^\infty \int_0^{2\pi} |\Psi|^2 r\, dr\, d\theta} \tag{4}$$

where $\Psi(r,\theta)$ is the electric field in the optical fiber, and $k = 2\pi/\lambda$. The electric field in the cladding is given by

$$\Psi_{\text{clad}}(r,\theta) = R_m(a) \frac{K_m(wr/a)}{K_m(w)} \frac{1}{\sqrt{2\pi}} e^{-jm\theta} \tag{5}$$

where m denotes the azimuthal mode number, K_m is the modified Hankel function of the order m, and w is a parameter defined as

$$w^2 = (\beta^2 - k^2 n_2{}^2)a^2. \tag{6}$$

We express the electric field in the core as

$$\Psi_{\text{core}}(r,\theta) = R_m(r) \frac{1}{\sqrt{2\pi}} e^{-jm\theta} \tag{7}$$

where $R_m(r)$ is expressed in terms of a set of orthogonal functions $F_{m,k}(r)$ as

$$R_m(r) = \sum_{k=1}^{L} C_k F_{mk}(r). \tag{8}$$

In the axially symmetric core,

$$F_{mk}(r) = \frac{\sqrt{2}}{a} \frac{J_m(\lambda_k r/a)}{J_m(\lambda_k)} \tag{9}$$

$$\lambda_k = \begin{cases} j_{1,k-1}, & \text{for } m = 0 \\ j_{m-1,k}, & \text{for } m \ne 0 \end{cases} \tag{10}$$

where $j_{m,k}$ denotes the kth root of $J_m(z) = 0$. These functions satisfy the orthonormalizing condition

$$\int_0^a F_{mk}(r) F_{ml}(r) r\, dr = \delta_{kl} \tag{11}$$

where δ_{kl} is Kronecker's delta. The continuity condition at the core–cladding interface $(r = a)$ is expressed approximately as [5][1]

$$\left[\frac{r}{\Psi_{\text{core}}} \frac{d\Psi_{\text{core}}}{dr}\right]_{r=a} = \left[\frac{r}{\Psi_{\text{clad}}} \frac{d\Psi_{\text{clad}}}{dr}\right]_{r=a} = \frac{wK_m'(w)}{K_m(w)}. \tag{12}$$

Putting (5), (7), and (12) into (4), and after some computations, we may express β^2 in terms of C_k as

$$\beta^2 = \left[\sum_{k=1}^{L}\sum_{l=1}^{L} C_k C_l (k^2 n_1{}^2 a^2 - \lambda_k{}^2)\delta_{kl} - v^2 \sum_{k=1}^{L}\sum_{l=1}^{L} C_k C_l A_{mkl} - \frac{2wK_{m-1}(w)}{K_m(w)} \sum_{k=1}^{L}\sum_{l=1}^{L} C_k C_l\right] \Big/ a^2 \sum_{k=1}^{L}\sum_{l=1}^{L} C_k C_l \delta_{kl} \tag{13}$$

where

$$A_{mkl} = \int_0^a g(r) F_{mk}(r) F_{ml}(r) r\, dr \tag{14}$$

$$v^2 = k^2 n_1{}^2 a^2 2\Delta. \tag{15}$$

From the condition that β^2 is stationary with respect to a small variation of Ψ, in other words to that of C_k, the following conditions must be satisfied for all k:

$$\frac{\partial \beta^2}{\partial C_k} = 0, \qquad k = 1,2,\cdots,L. \tag{16}$$

Using (13) and (16), we obtain

$$\sum_{l=1}^{L} C_l S_{kl} = 0, \qquad k = 1,2,\cdots,L \tag{17}$$

where

$$S_{kl} = -\frac{2wK_{m-1}(w)}{K_m(w)} + (u^2 - \lambda_k{}^2)\delta_{kl} - v^2 A_{mkl} \tag{18}$$

$$u^2 = (k^2 n_1{}^2 - \beta^2)a^2 = v^2 - w^2. \tag{19}$$

In order that a nontrivial solution of (17) exists,

$$\det (S_{kl}) = 0 \tag{20}$$

must hold. This equation is the characteristic equation which determines the propagation constant of an optical fiber.

[1] An approximation $(1 - n(a)/n_2) \simeq 0$ is used in deriving (12). Therefore, when a step or valley is present at the core–cladding boundary, a small error will be introduced by using (12). However, in most practical cases we may approximate $(1 - n(a)/n_2) \to 0$ (weak guidance approximation) and use (12).

B. Delay Time

The variational expression of the propagation constant [see (4)] is stationary with respect to a small variation of Ψ. Therefore, we may find $d\beta/dk$ by differentiating (4) only where k appears explicitly (see Appendix I). Thus we obtain

$$\beta \frac{d\beta}{dk} = \frac{\int_0^\infty \int_0^{2\pi} kn \frac{d(kn)}{dk} |\Psi|^2 r\, dr\, d\theta}{\int_0^\infty \int_0^{2\pi} |\Psi|^2 r\, dr\, d\theta}. \tag{21}$$

Putting (2), (5), and (7) into (21), we obtain

$$\frac{\beta}{kn_1}\frac{d\beta}{dk} = N_1 \left\{1 - \Delta\left(2 + \frac{y}{2}\right) \frac{\int_0^\infty \int_0^{2\pi} g(r)|\Psi|^2 r\, dr\, d\theta}{\int_0^\infty \int_0^{2\pi} |\Psi|^2 r\, dr\, d\theta}\right\}$$

$$= N_1 \left\{1 - \Delta\left(2 + \frac{y}{2}\right) \cdot \frac{\sum_{k=1}^{L}\sum_{l=1}^{L} C_k C_l [A_{mkl} + 1/\xi_m - 1]}{\sum_{k=1}^{L}\sum_{l=1}^{L} C_k C_l [\delta_{kl} + 1/\xi_m - 1]}\right\} \tag{22}$$

where

$$\xi_m = \frac{K_m^2(w)}{K_{m-1}(w)K_{m+1}(w)} \tag{23a}$$

$$N_1 = \frac{d(kn_1)}{dk} \tag{23b}$$

$$y = -\frac{2n_1}{N_1}\frac{\lambda}{\Delta}\frac{d\Delta}{d\lambda}. \tag{23c}$$

Among the preceding parameters, N_1 is the group index [1], and y is a parameter representing the difference in material dispersions in the core and the cladding [2]; typically, $y = 0.3$. From (15) and (19), β is given by

$$\beta = kn_1 \left(1 - 2\Delta \frac{u^2}{v^2}\right)^{1/2}. \tag{24}$$

Thus from (22) and (24), the delay time per unit length $\tau(\omega)$ may be expressed as

$$\tau \triangleq \frac{d\beta}{d\omega} = \frac{N_1}{c} \frac{[1 - \Delta(2 + y/2)\Theta]}{[1 - 2\Delta u^2/v^2]^{1/2}} \tag{25}$$

where c denotes the light velocity in the free space, and

$$\Theta = \frac{\sum_{k=1}^{L}\sum_{l=1}^{L} C_k C_l [A_{mkl} + 1/\xi_m - 1]}{\sum_{k=1}^{L}\sum_{l=1}^{L} C_k C_l [\delta_{kl} + 1/\xi_m - 1]}. \tag{26}$$

The matrix element A_{mkl} is given, from (3), (9), and (14), as

$$A_{mkl} = \sum_{p=1}^{n} \kappa_p D_{pmkl} \tag{27}$$

where

$$D_{pmkl} = H_{pmkl} - \left(\frac{r_0}{a}\right)^{2p} \delta_{kl} \tag{28}$$

$$H_{pmkl} = 2\int_0^1 x^{2p} \frac{J_m(\lambda_k x)J_m(\lambda_l x)}{J_m(\lambda_k)J_m(\lambda_l)} x\, dx. \tag{29}$$

The value of H_{pmkl} is independent from κ_p. We may therefore calculate those matrix elements before we start the synthesis of the optimum refractive-index profile.

IV. Synthesis of the Optimum Refractive-Index Profile

A. Measure of Multimode Dispersion

As the measure of the multimode dispersion at frequencies where M modes propagate, we define

$$Q(M) = \frac{\int_{v_{c,M}+\varepsilon}^{v_{c,M+1}-\varepsilon} \sigma(v)\, dv}{\int_{v_{c,M}+\varepsilon}^{v_{c,M+1}-\varepsilon} dv} \tag{30}$$

where ε is a small quantity and $\sigma(v)$ is the variance of the delay time for the M modes;

$$\sigma(v) = \frac{1}{M}\sum_{i=1}^{M} [\tau_i(v) - \langle\tau(v)\rangle]^2. \tag{31}$$

In the preceding equation,

$$\langle\tau(v)\rangle = \frac{1}{M}\sum_{i=1}^{M} \tau_i(v) \tag{32}$$

$\tau_i(v)$ is the delay time of the ith mode expressed in terms of the normalized frequency, and $v_{c,M}, v_{c,M+1}$ are normalized cutoff frequencies of the Mth mode and the $(M+1)$th mode, respectively. In defining the measure $Q(M)$, the variance is averaged between two cutoff frequencies because it is practically difficult to choose a specific transmission frequency with respect to (for example, at the median of) two cutoff frequencies.

We consider that the optimum refractive-index profile of an optical fiber transmitting M modes is given by the condition making $Q(M)$ minimum. Therefore, it is obtained as a solution of a simultaneous equation

$$\frac{\partial Q(M)}{\partial \kappa_p} = 0, \qquad p = 1,2,\cdots,n. \tag{33}$$

B. Routine of the Synthesis

The flow chart (Fig. 2) shows the routine of the synthesis.

C. Modification of κ_p by Newton–Raphson Method

As shown at the bottom of Fig. 2, the Newton–Raphson method [8] is used in the modification of κ_p. This method will first be described for a single scalar equation. Suppose the numerical solution of an equation

$$G(\kappa) = 0 \tag{34}$$

is to be obtained. In the Newton–Raphson method, we first assume a proper initial value κ_i and modify κ according to a relation

$$\kappa_{h+1} = \kappa_h - \frac{G(\kappa_h)}{G'(\kappa_h)} d \tag{35}$$

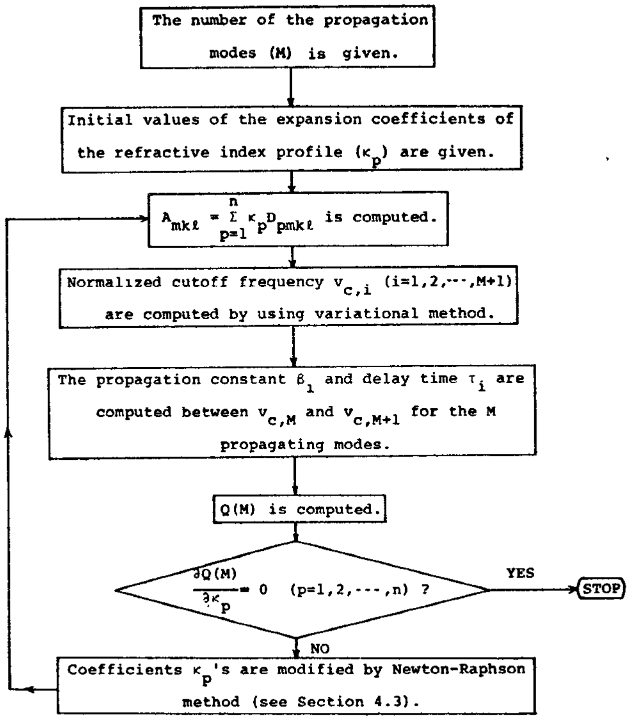

Fig. 2. Routine of the synthesis of the optimum refractive-index profile.

where h denotes the number of repetitions and d is a deceleration factor for preventing oscillation of the solution.

In the present case, the solution of a simultaneous equation

$$G(\kappa) = \begin{pmatrix} G_1(\kappa) \\ G_2(\kappa) \\ \vdots \\ G_n(\kappa) \end{pmatrix} = 0 \qquad (36)$$

must be obtained, where $\kappa = (\kappa_1, \kappa_2, \cdots, \kappa_n)^T$. In this case the modification formula corresponding to (35) is given as

$$\kappa_{h+1} = \kappa_h - dJ^{-1}(\kappa_h)G(\kappa_h). \qquad (37)$$

In the preceding equation J^{-1} is the inverse matrix of J, which is the Jacobian of $G(\kappa)$ with respect to κ:

$$J(\kappa) = \begin{pmatrix} J_{11}(\kappa) & \cdots & J_{1n}(\kappa) \\ \vdots & & \vdots \\ J_{n1}(\kappa) & \cdots & J_{nn}(\kappa) \end{pmatrix} \qquad (38)$$

where

$$J_{pq}(\kappa) = \frac{\partial G_p(\kappa)}{\partial \kappa_q}, \qquad p,q = 1,2,\cdots,n. \qquad (39)$$

Under proper conditions, κ_h converges to the solution of (36), which satisfies

$$J^{-1}(\kappa)G(\kappa) = 0 \qquad (40a)$$

$$\kappa_{h+1} - \kappa_h \to 0. \qquad (40b)$$

In the present problem, each line of the simultaneous equation (36) is given, from (33), as

$$G_p(\kappa) = \frac{\partial Q(M)}{\partial \kappa_p}, \qquad p = 1,2,\cdots,n. \qquad (41)$$

[In the actual computation of $Q(M)$, the integrals in (30) are replaced by summations to save the computer time. That is, we choose N sampling points v_j ($j = 1,2,\cdots,N$) between $v_{c,M}$ and $v_{c,M+1}$ and use

$$Q(M) = \frac{1}{N}\sum_{j=1}^{N} \sigma(v_j) \qquad (42)$$

as the approximate measure of the multimode dispersion instead of (30).] Therefore, each element of $G(\kappa)$ and $J(\kappa)$ is given, from (39), (41), and (42), as

$$G_p(k) = \frac{1}{N}\sum_{j=1}^{N} \frac{\partial \sigma(v_j)}{\partial \kappa_p}, \qquad (43)$$

$$J_{pq}(k) = \frac{1}{N}\sum_{j=1}^{N} \frac{\partial^2 \sigma(v_j)}{\partial \kappa_q \partial \kappa_p}, \qquad p,q = 1,2,\cdots,n. \qquad (44)$$

The details of the computation of $G_p(\kappa)$ and $J_{pq}(\kappa)$ are described in Appendix II [see (A20) and (A24)]. Putting those values into (37), we may compute κ_{h+1} from κ_h. Repetition of such a process finally leads to the optimum κ, that is, the optimum set of κ_p.

V. Results

To show the feasibility of the preceding process, an example of the synthesis will be described for the following parameters:

$M = 10$ (M: number of propagating linearly polarized (LP) modes[2]);
$n = 5$ (n: number of terms representing the refractive-index profile);
$N = 3$ (N: number of sampling points between $v_{c,10}$ and $v_{c,11}$);
$L = 10$ (L: number of terms representing the electric field in the core);
$y = 0.3$ (y: difference in material dispersions in the core and the cladding);
$n_1 = 1.5$ (n_1: maximum refractive index in the core);
$\Delta = 0.01$ (Δ: see (1)).

The starting profile is a "quadratic distribution with a valley having depth equal to half the peak" (that is, $\kappa_1 = 1.5$, $\kappa_2 = \kappa_3 = \kappa_4 = \kappa_5 = 0$). Such a profile has been claimed by the present authors to be a fairly good one as far as α-power refractive-index distributions in the core are considered [3].

The gradual change of the profile is shown in Fig. 3, where the abscissa h denotes the number of repetitions performed. The corresponding variation of the normalized delay time between $v_{c,10}$ and $v_{c,11}$ is shown in Fig. 4. The variations of maximum delay difference between modes ($\delta\tau_{MAX}$) and the square root of the measure $Q(M)$ defined by (30) are shown in Fig. 5(b). It is found that both $\delta\tau_{MAX}$ and $\sqrt{Q(M)}$ are reduced dramatically; it is reduced to about 3×10^{-3} times the starting value. Note that the

[2] The total number of the degenerated modes (having different polarizations and/or field configurations) included in the 10 LP modes is 34.

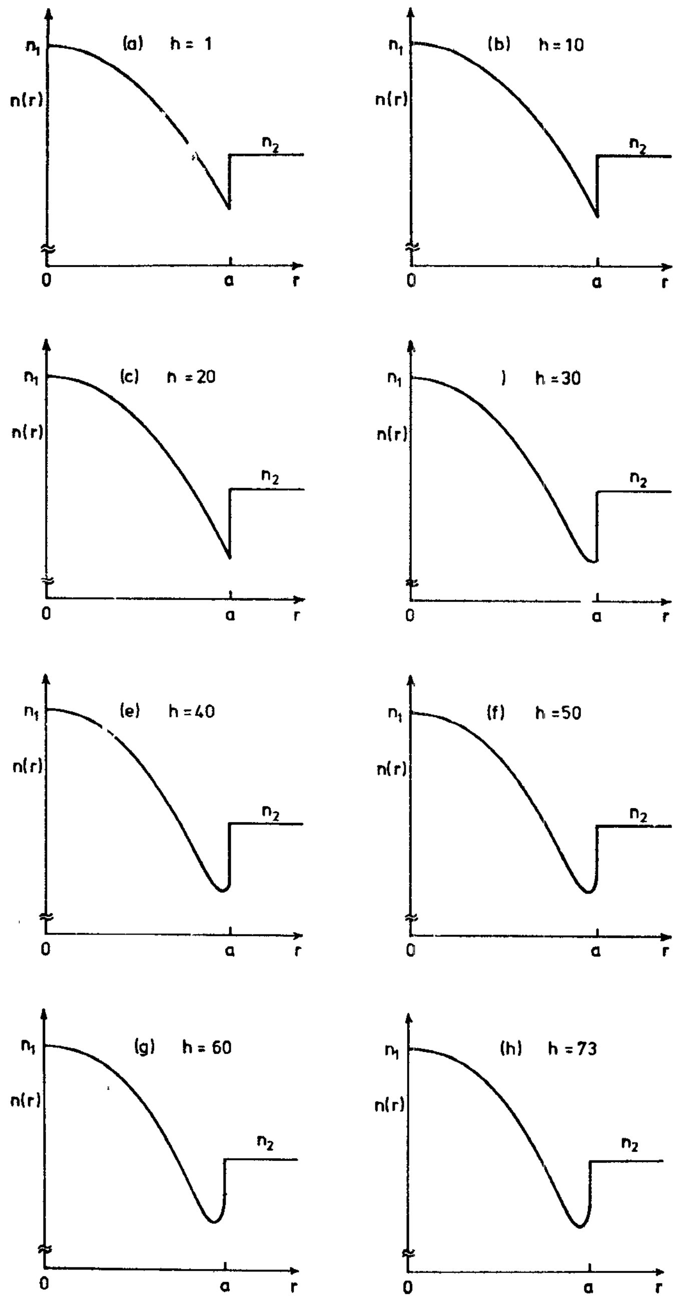

Fig. 3. Variation of the refractive-index profile. Initial profile is a quadratic with step ($\kappa_1 = 1.5, \kappa_2 = \kappa_3 = \kappa_4 = \kappa_5 = 0$).

starting value itself is much lower than the value obtained with a uniform-core fiber. The typical values of $\delta\tau_{\text{MAX}}$ for $M = 10$ are approximately 30000 ps/km for the uniform-core fiber, 14000 ps/km for the starting profile,[3] and 30 ps/km for the really optimized profile. The last value is comparable to the material dispersion obtained with an ordinary silica fiber and a typical semiconductor laser with a wavelength spread of 0.2 nm; for such a combination $\delta\tau_{\text{material}}$ is typically 20 ps/km.

The variations of the expansion coefficients are shown in Fig. 5(a) as functions of h. It is found that the coefficients for higher order terms (for x^6, x^8, x^{10}) drastically increases, but the resultant profiles are apparently similar to the original. The principal difference is that the sharp valley is smoothed.

The computer time required was about 20 s for one cycle of the analysis, estimation, and modification, when HITAC 8700/8800 was used.

VI. Discussions

1) In the preceding section, an example of the synthesis has been described for an optical fiber in which ten modes propagate. Of course, the same methods may be used for any number of modes M. However, the computer time required is proportional to M^2.

2) A possible trouble inherent to such a trial-and-error optimization is the presence of many optima, that is, the possibility of arriving at different "optimum" profiles when the starting profiles are different. Mathematically, such a possibility cannot be denied in the present case. However, another trial-and-error synthesis starting from a different profile ($\kappa_1 = 1.0, \kappa_2 = \kappa_3 = \kappa_4 = \kappa_5 = 0$) finally led to an optimum profile the same as Fig. 3(h). The authors believe that the same profile is obtained unless we start from an intentionally peculiar (for example, sawtoothlike) profile.

3) In Fig. 5(b) the readers might notice a sudden decrease of the dispersion at $h = 14$. Such a phenomenon is sometimes encountered in the Newton–Raphson solution; it is due to an accidental, lucky coincidence. Note that the expansion coefficients do not show any drastic change at $h = 14$.

4) We should note that the dispersion is reduced by 10^{-1} between $h = 50$ and $h = 70$, whereas the profiles show very little difference between them. In the present state-of-the-art, such a little difference of the profile can never be controlled. Establishment of a very fine profile-control technique [probably a computer-controlled chemical vapor deposition (CVD) technique] is desired.

5) By the curve-fitting method, it was found that the optimum refractive-index profile can be approximated as

$$n^2(r) = n_1^2[1 - 4.00\Delta(r/a)^{2.27}]$$

for $0 \leq r/a \leq 0.9$, when $y = 0.3$. On the other hand, when $y = 0.0$, the approximate profile is given as

$$n^2(r) = n_1^2[1 - 4.04\Delta(r/a)^{1.97}]$$

for $0 \leq r/a \leq 0.9$. These approximate formulas are in good agreement with Olshansky and Keck's result [2].

6) To demonstrate the effectiveness of the refractive-index valley at the core–cladding boundary, values of $\sqrt{Q(M)}$ of quadratic-core fibers have been computed for various M as functions of the valley depth. Fig. 6(a) shows $\sqrt{Q(M)}$ as functions of the parameter ρ representing the valley depth (see [3]). It is found that the deeper the valley, the smaller the value of $\sqrt{Q(M)}$. In Fig. 6(b), cases are compared when the valley is filled up to various levels. It is found that a minimum point is present for ρ_0. In the case of $M = 10$,

[3] This value may seem too large; the reason is that the highest order mode is included in the calculation of $\delta\tau_{\text{MAX}}$. If we exclude the highest order mode, $\delta\tau_{\text{MAX}}$ is 25 000 ps/km for the uniform-core fiber and 3000 ps/km for the starting profile.

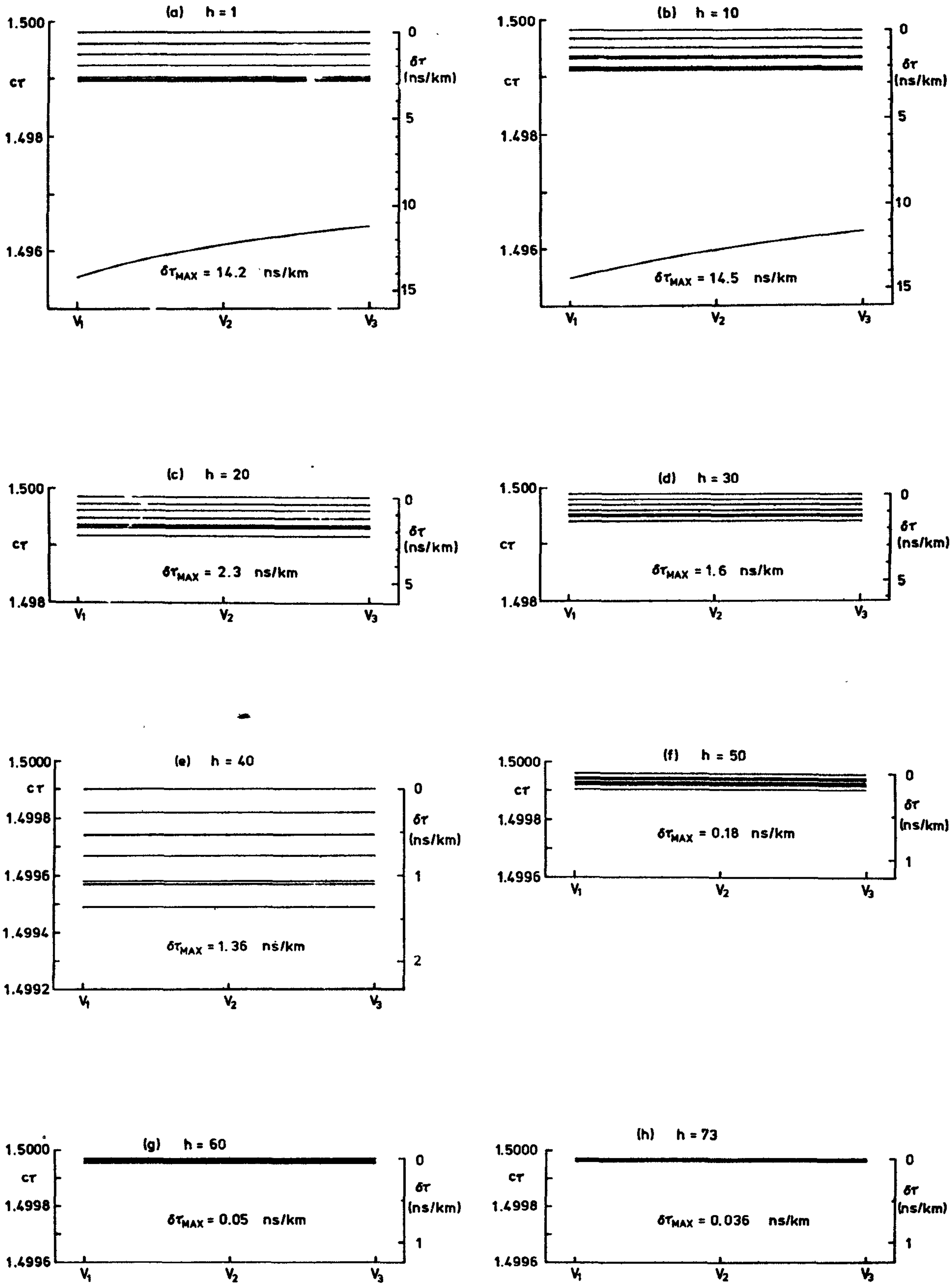

Fig. 4. Variation of the normalized delay time. Note that the ordinate is expanded in (e)–(h).

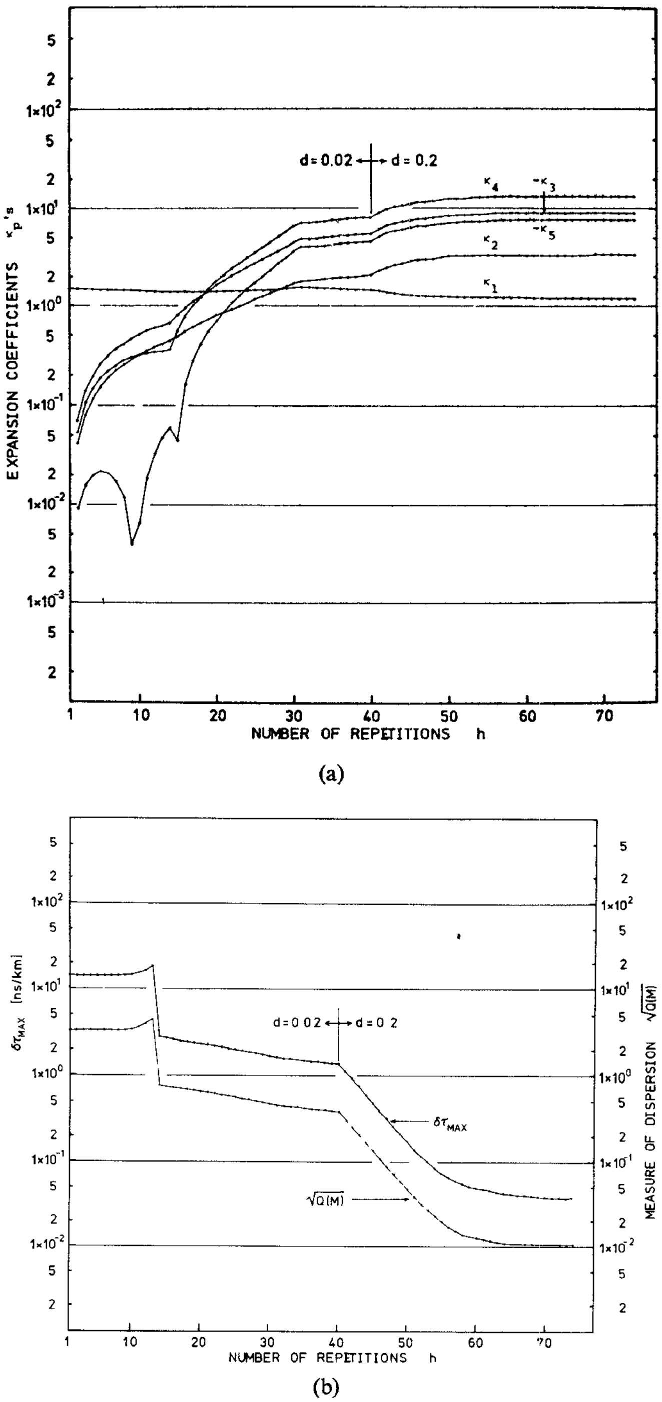

Fig. 5. Variation of (a) the expansion coefficients (κ_p) and (b) the square root of the measure of the multimode dispersion ($\sqrt{Q(M)}$) and the maximum value of the mode delay difference ($\delta\tau_{MAX}$).

for which the synthesis has been performed, the minimum is found at $\rho_0 \fallingdotseq 1.5$, which gives a good approximation to the optimum profile obtained by the synthesis [see Fig. 3(h)].

VII. Conclusion

The optimum refractive-index profile of a multimode fiber has been obtained by a computer-aided trial-and-error synthesis method. The proposed method will be useful for the design of multimode optical fibers.

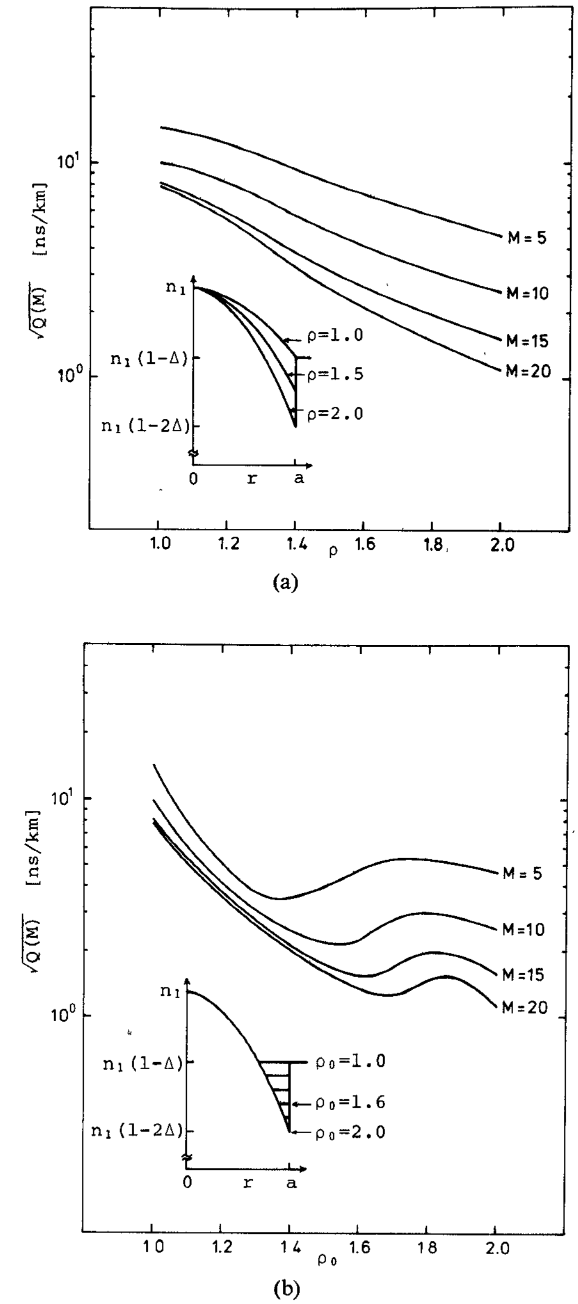

Fig. 6. The measure $\sqrt{Q(M)}$ of quadratic core fiber for various M; (a) as functions of the valley depth, (b) as functions of the level to which the valley is filled up.

Appendix I
Derivation of (21) [9]

We first note that the right-hand side of (4) is stationary for a small variation of $\Psi(r,\theta)$. When k deviates slightly making β and Ψ also deviate, we have

$$(\beta + \delta\beta)^2 \int_s |\Psi + \delta\Psi|^2 \, dS - \int_s [kn + \delta(kn)]^2 |\Psi + \delta\Psi|^2 \, dS - \int_s |\nabla\Psi + \delta\nabla\Psi|^2 \, dS = 0 \quad \text{(A1)}$$

where $\int_s dS$ denotes the integral over the cross section of the fiber. Neglecting the terms of order δ^2, we may rewrite (A1) as

$$\left\{\beta^2 \int_s |\Psi|^2\, dS - \int_s k^2 n^2 |\Psi|^2\, dS + \int_s |\nabla\Psi|^2\, dS\right\} + \left\{\beta^2 \int_s \delta|\Psi|^2\, dS - \int_s k^2 n^2 \delta|\Psi|^2\, dS + \int_s \delta|\nabla\Psi|^2\, dS\right\} + \left\{2\beta\delta\beta \int_s |\Psi|^2\, dS - 2\int_s kn\delta(kn)|\Psi|^2\, dS\right\} = 0. \quad \text{(A2)}$$

Applying the stationary condition $\delta\beta^2 = 0$, that is,

$$\beta^2 \int_s \delta|\Psi|^2\, dS - \int_s k^2 n^2 \delta|\Psi|^2\, dS + \int_s \delta|\nabla\Psi|^2\, dS = 0 \quad \text{(A3)}$$

to the second term of (A2), and also applying (4) to the first term of (A2), we obtain

$$\beta\delta\beta \int_s |\Psi|^2\, dS - \int_s kn\delta(kn)|\Psi|^2\, dS = 0. \quad \text{(A4)}$$

Equation (A4) may be rewritten as

$$\beta \frac{d\beta}{dk} = \frac{\displaystyle\int_s kn \frac{d(kn)}{dk} |\Psi|^2\, dS}{\displaystyle\int_s |\Psi|^2\, dS}. \quad \text{(A5)}$$

Appendix II
Derivation of Equations Giving $G_p(\kappa)$ and $J_{pq}(\kappa)$

From (22), delay time τ is expressed as

$$\tau = \frac{kn_1 N_1}{c\beta}\left\{1 - \Delta\left(2 + \frac{y}{2}\right)\frac{\int_s g(r)|\Psi|^2\, dS}{\int_s |\Psi|^2\, dS}\right\}. \quad \text{(A6)}$$

Partially differentiating τ with respect to κ_p, $\partial\tau/\partial\kappa_p$ is given

$$\frac{\partial\tau}{\partial\kappa_p} = \frac{\Delta N_1}{c} T_p, \qquad p = 1,2,\cdots,n \quad \text{(A7)}$$

where

$$T_p = \left(2 + \frac{y}{2}\right)\frac{\displaystyle\sum_{k=1}^{L}\sum_{l=1}^{L}\left(C_k \frac{\partial C_l}{\partial\kappa_p} + C_l \frac{\partial C_k}{\partial\kappa_p}\right)\{\Theta[\delta_{kl} + 1/\xi_m - 1] - [A_{mkl} + 1/\xi_m - 1]\}}{\displaystyle\sum_{k=1}^{L}\sum_{l=1}^{L} C_k C_l[\delta_{kl} + 1/\xi_m - 1]} - \left(1 + \frac{y}{2}\right)\frac{\displaystyle\sum_{k=1}^{L}\sum_{l=1}^{L} C_k C_l D_{pmkl}}{\displaystyle\sum_{k=1}^{L}\sum_{l=1}^{L} C_k C_l[\delta_{kl} + 1/\xi_m - 1]}. \quad \text{(A8)}$$

In the preceding calculation, it is assumed that n_1 and Δ do not change in the course of the optimization.

The term $\partial C_l/\partial\kappa_p$ in (A8) can be calculated as follows. From (17) and the normalizing condition for the power density, we have

$$\boldsymbol{SC} = \boldsymbol{0} \quad \text{(A9)}$$

$$\boldsymbol{C}^T\boldsymbol{WC} = 1 \quad \text{(A10)}$$

where $\boldsymbol{C}$ is an L-element column vector consisting of C_k in (8), and $\boldsymbol{S}$ and $\boldsymbol{W}$ are $L \times L$ matrices:

$$S_{kl} = -\frac{2wK_{m-1}(w)}{K_m(w)} + (u^2 - \lambda_k^2)\delta_{kl} - v^2 A_{mkl} \quad \text{(A11)}$$

$$W_{kl} = \delta_{kl} + 1/\xi_m - 1. \quad \text{(A12)}$$

Partially differentiating (A9) and (A10) with respect to κ_p $(p = 1,2,\cdots,n)$, we obtain

$$\boldsymbol{S}^*\boldsymbol{C} + \boldsymbol{SC}^* = \boldsymbol{0} \quad \text{(A13)}$$

$$\tfrac{1}{2}\boldsymbol{C}^T\boldsymbol{W}^*\boldsymbol{C} + \boldsymbol{C}^T\boldsymbol{WC}^* = 0 \quad \text{(A14)}$$

where the symbol * denotes a differentiation with respect to κ_p. We may combine (A13) and (A14) to obtain

$$\boldsymbol{AC}^* = -\boldsymbol{BC} \quad \text{(A15)}$$

where $\boldsymbol{A}$ and $\boldsymbol{B}$ are $(L + 1) \times L$ matrices given as

$$\boldsymbol{A} = \begin{pmatrix} \boldsymbol{S} \\ \boldsymbol{C}^T\boldsymbol{W} \end{pmatrix} \quad \text{(A16)}$$

$$\boldsymbol{B} = \begin{pmatrix} \boldsymbol{S}^* \\ \tfrac{1}{2}\boldsymbol{C}^T\boldsymbol{W}^* \end{pmatrix}. \quad \text{(A17)}$$

By using the generalized inverse matrix of $\boldsymbol{A}$ which is expressed as

$$\boldsymbol{A}^- = \boldsymbol{A}^T(\boldsymbol{AA}^T)^{-1} \quad \text{(A18)}$$

$\boldsymbol{C}^*$ is given, from (A15) and (A18), as

$$\boldsymbol{C}^* = -\boldsymbol{A}(\boldsymbol{AA}^T)^{-1}\boldsymbol{BC}. \quad \text{(A19)}$$

Putting (31), (32), (42), and (A7) into (41), we obtain

$$G_p(\kappa) = \langle\!\langle \Gamma T_p \rangle\!\rangle - \langle\!\langle \Gamma \rangle\langle T_p \rangle\!\rangle \quad \text{(A20)}$$

where

$$\Gamma = \frac{u^2}{v^2} - \left(2 + \frac{y}{2}\right)\Theta \quad \text{(A21)}$$

$$\langle\!\langle \Gamma T_p \rangle\!\rangle = \frac{1}{N}\sum_{j=1}^{N}\left[\frac{1}{M}\sum_{i=1}^{M}\Gamma_{ij}T_{ijp}\right] \quad \text{(A22)}$$

$$\langle\!\langle \Gamma \rangle\langle T_p \rangle\!\rangle = \frac{1}{N}\sum_{j=1}^{N}\left[\frac{1}{M}\sum_{i=1}^{M}\Gamma_{ij}\right]\left[\frac{1}{M}\sum_{i=1}^{M}T_{ijp}\right]. \quad \text{(A23)}$$

We may also obtain J_{pq} from (31), (32), (43), and (A7) as

$$J_{pq}(\kappa) = \langle\!\langle T_p T_q \rangle\!\rangle - \langle\!\langle T_p \rangle\langle T_q \rangle\!\rangle \quad \text{(A24)}$$

where

$$\langle\!\langle T_p T_q \rangle\!\rangle = \frac{1}{N}\sum_{j=1}^{N}\left[\frac{1}{M}\sum_{i=1}^{M}T_{ijp}T_{ijq}\right] \quad \text{(A25)}$$

$$\langle\!\langle T_p \rangle\langle T_q \rangle\!\rangle = \frac{1}{N}\sum_{j=1}^{N}\left[\frac{1}{M}\sum_{i=1}^{M}T_{ijp}\right]\left[\frac{1}{M}\sum_{i=1}^{M}T_{ijq}\right]. \quad \text{(A26)}$$

In (A20) and (A24), G_p and J_{pq} are normalized by $2(\Delta N_1/c)^2$.

ACKNOWLEDGMENT

The authors wish to thank F. Kato of the University of Tokyo for his helpful suggestions concerning the application of the Newton–Raphson method.

REFERENCES

[1] D. Gloge and E. A. J. Marcatili, "Multimode theory of graded-core fibers," *Bell Syst. Tech. J.*, vol. 52, pp. 1563–1578, Nov. 1973.
[2] R. Olshansky and D. B. Keck, "Pulse broadening in graded-index optical fibers," *Appl. Opt.*, vol. 15, pp. 483–491, Feb. 1976.
[3] K. Okamoto and T. Okoshi, "Analysis of wave propagation in optical fibers having core with α-power refractive-index distribution and uniform cladding," *IEEE Trans. Microwave Theory Tech.*, vol. MTT-24, pp. 416–421, July 1976.
[4] S. Geckeler, "Dispersion in optical waveguides with graded refractive index," *Electron Lett.*, vol. 11, pp. 139–140, Apr. 1975.
[5] T. Okoshi and K. Okamoto, "Analysis of wave propagation in inhomogeneous optical fibers using a variational method," *IEEE Trans. Microwave Theory Tech.*, vol. MTT-22, pp. 938–945, Nov. 1974.
[6] Y. Suematsu and K. Furuya, "Quasi-guided modes and related radiation losses in optical dielectric waveguides with external higher index surroundings," *IEEE Trans. Microwave Theory Tech.*, vol. MTT-23, pp. 170–175, Jan. 1975.
[7] K. Kurokawa, "Electromagnetic waves in waveguides with wall impedance," *IRE Trans. Microwave Theory Tech.*, vol. MTT-10, pp. 314–320, Sept. 1962.
[8] F. Kato, M. Saito, and T. Okoshi, "Computer-aided synthesis of planar circuits," to be published.
[9] K. M. Case, "On wave propagation in inhomogeneous media," *J. Math. Phys.*, vol. 13, p. 360, Mar. 1972.

Short Papers

Propagation in Circular Waveguide Loaded with an Azimuthally Magnetized Ferrite Tube

OLIVIER PARRIAUX AND FRED E. GARDIOL, SENIOR MEMBER, IEEE

***Abstract*—A new computer method for the study of radially inhomogeneous guiding structures presenting circular symmetry is utilized to determine propagation properties of a ferrite loaded guide. The nonreciprocal characteristics obtained can be used to design latching rotators and differential phase shifters for polarization orthogonality restoration in high-frequency (above 10 GHz) communication systems with frequency reuse.**

I. INTRODUCTION

A circular waveguide loaded with one or several tubes of azimuthally magnetized ferrite supports nonreciprocal modes of propagation, which may be used to realize rotators and differential phase shifters. This possibility was briefly outlined by Fox *et al.* [1] and by Clarricoats [2].

Until now, however, the studies devoted to this guiding structure only considered TE_{0n} modes, for which an exact analytical solution is available in terms of hypergeometric functions [3]–[6]. A perturbation method also developed for this structure was applied only to study TE_{0n} mode propagation [7]. It must be noted, however, that the dominant mode of the empty circular waveguide is the TE_{11} mode, which is not part of the TE_{0n} mode subset; the mode hierarchy remains basically the same for low to medium loading of the waveguide, i.e., conditions most suitable for device operation. Only when the waveguide is more heavily loaded with dielectric inserts does the mode inversion described by Tsandoulas and Ince [8], [9] take place: The TE_{01} mode then becomes the dominant mode. By using a circular waveguide with dielectric loading, results available for TE_{01} propagation could thus be utilized in the design of devices [10]. Partial studies only are available in the technical literature, due to the lack of a mathematical method capable of solving the field problem for hybrid modes.

In practical device development, however, a more complete knowledge of the mode structure is necessary; the propagation properties of the dominant mode must be known in order to design the device, while the cutoff frequency of the first higher order mode limits the frequency range suitable for operation.

A computation technique, based on the application of a one-dimensional finite-difference approach, was recently developed by the authors [11]. This new approach yields the propagation constant and the field pattern for any mode in a radially inhomogeneous cylindrical structure presenting circular symmetry, of which the ferrite loaded circular waveguide considered here is one example.

The presence of azimuthally magnetized ferrite in the circular waveguide produces a difference between the propagation characteristics of the first two normal modes propagating in the structure, which are respectively right hand and left hand circularly polarized (in nongyrotropic circularly symmetrical structures, these two modes are spatially degenerate). When a linearly polarized wave travels through a section of loaded guide, its plane of polarization is rotated in the same manner as it is in longitudinally magnetized Faraday rotators [12]. The addition of quarter-wave plates at both ends allows one to realize a polarization-dependent phase shifter; the principle of operation is the same as the one used by Boyd [13], with the following differences:

1) The center section makes use of an azimuthally magnetized ferrite tube instead of a Faraday rotator, which requires an external magnetic circuit.

2) Both device ends are connected to circular waveguide.

Manuscript received April 2, 1976; revised July 19, 1976. This work was supported by the Swiss National Science Foundation under Grant 2, 346, 0, 75.

O. Parriaux was with the Chaire d'Electromagnétisme et d'Hyperfréquences, École Polytechnique Fédérale, Lausanne, Switzerland. He is now with the Department of Electrical and Electronics Engineering, University College London, London, England.

F. E. Gardiol is with the Chaire d'Electromagnétisme et d'Hyperfréquences, École Polytechnique Fédérale, Lausanne, Switzerland.